

## Influence of heat treatment on the structure and corrosion properties of microalloyed pipe steels with a chromium content of up to 1 %

*Elena A. Chistopoltseva*<sup>\*1,5</sup>, PhD (Engineering),  
Head of Department of Special Materials Science  
*Dmitry V. Kudashov*<sup>2,6</sup>, PhD (Engineering), Director  
*Aleksandr A. Komissarov*<sup>3,7</sup>, PhD (Engineering),  
Head of Hybrid Nanostructured Materials Laboratory  
*Vyacheslav V. Yushchuk*<sup>3,8</sup>, scientific project engineer  
*Aleksandr V. Muntin*<sup>4</sup>, PhD (Engineering),  
Director of Engineering and Technology Center  
*Aleksey V. Chervonniy*<sup>4</sup>, PhD (Engineering),  
Head of Research and Development Department  
*Egor D. Dolgach*<sup>3</sup>, scientific project engineer

<sup>1</sup>LLC IT Service, Samara (Russia)

<sup>2</sup>Vyksa branch of MISIS University of Science and Technology, Vyksa (Russia)

<sup>3</sup>MISIS University of Science and Technology, Moscow (Russia)

<sup>4</sup>JSC Vyksa Metallurgical Plant, Vyksa (Russia)

\*E-mail: chistopolceva@its-samara.com

<sup>5</sup>ORCID: <https://orcid.org/0009-0002-5587-287X>

<sup>6</sup>ORCID: <https://orcid.org/0000-0002-7661-1591>

<sup>7</sup>ORCID: <https://orcid.org/0000-0002-8758-5085>

<sup>8</sup>ORCID: <https://orcid.org/0000-0002-3015-1235>

Received 22.04.2025

Revised 20.05.2025

Accepted 17.07.2025

**Abstract:** The service life of oil pipelines has recently decreased significantly due to severe operating conditions and the increased aggressiveness of the environment, caused by the simultaneous presence of dissolved hydrogen sulfide, carbon dioxide, chlorides, and a high water phase content. Conventional corrosion mitigation methods typically address only one of these factors and therefore fail to provide adequate protection under such combined conditions. This limitation necessitates the use of multiple complementary approaches for corrosion control. This paper proposes microalloying systems for low-carbon steels of grades 10KhB, 10F, 10B, and 15KhF (with chromium content up to 1 %) for seamless pipes, along with optimized heat treatment regimes that provide increased strength, cold resistance, and corrosion resistance in CO<sub>2</sub>- and H<sub>2</sub>S-containing environments. Mechanical testing after heat treatment demonstrated that the proposed chemical compositions ensure strength classes K52–K56, while also providing high low-temperature toughness. The morphology of carbides in the microstructure depends on the chemical composition and determines the steel's strength, though it does not affect corrosion resistance. The investigated steels showed high resistance to hydrogen-induced cracking (HIC) and sulfide stress cracking (SSC). After exposure to CO<sub>2</sub>–H<sub>2</sub>S media, a protective iron sulfide film formed on the surface, indicating uniform sulfide corrosion. The corrosion rate and mechanism were found to be governed by the medium composition and the kinetics of iron sulfide film formation. The obtained results allow expanding the scope of application of the proposed steels in multicomponent aggressive environments regardless of the type of microalloying.

**Keywords:** low-carbon microalloyed steel; heat treatment; corrosion-resistant seamless pipe; CO<sub>2</sub>- and H<sub>2</sub>S-containing environment; sulfide corrosion of steel; fine-grained structure; oilfield pipelines.

**Acknowledgments:** The work was carried out within a comprehensive project on the topic “Development and Implementation of Integrated Technologies for the Production of Seamless Pipes from New-Generation Steels with Controlled Corrosion Resistance under Abnormal Operating Conditions for the Fuel and Energy Complex of the Russian Federation” within the agreements No. 075-11-2023-011 dated 10.02.2023 and No. 075-11-2025-017 dated 27.02.2025 in accordance with RF Government Resolution No. 218 dated 09.04.2010.

**For citation:** Chistopoltseva E.A., Kudashov D.V., Komissarov A.A., Yushchuk V.V., Muntin A.V., Chervonniy A.V., Dolgach E.D. Influence of heat treatment on the structure and corrosion properties of microalloyed pipe steels with a chromium content of up to 1 %. *Frontier Materials & Technologies*, 2025, no. 3, pp. 101–111. DOI: 10.18323/2782-4039-2025-3-73-8.

© Chistopoltseva E.A., Kudashov D.V., Komissarov A.A.,  
Yushchuk V.V., Muntin A.V., Chervonniy A.V., Dolgach E.D., 2025

## INTRODUCTION

Metal corrosion resulting from the transported medium is the main cause of failures in oil field pipelines. According to [1; 2], the presence of simultaneously dissolved hydrogen sulfide ( $H_2S$ ) and carbon dioxide ( $CO_2$ ), even in small concentrations, significantly accelerates corrosion processes, leading to premature wear of equipment, reduced reliability and emergency situations. The partial pressure of gases  $pH_2S$  and  $pCO_2$  affects the rate of chemical and electrochemical reactions, the degree of hydrogenation of steel and the likelihood of stress corrosion cracking.

Aggressive environments typical for oil and gas production contain water, dissolved salts, carbon dioxide, hydrogen sulfide and organic acids that actively destroy metal. There are several types of corrosion, the most common of which are general, pitting, crevice, sulfide, and stress corrosion cracking. An integrated approach, including several areas, is required to protect effectively equipment from corrosion. Firstly, it is important to choose the right materials that are resistant to specific operating conditions. Stainless steels and alloys, polymeric materials are widely used in the manufacture of pipes, fittings, tanks and other equipment. Secondly, the use of corrosion inhibitors is an effective way to slow down corrosion processes by forming a protective layer that prevents metal from coming into contact with the environment [3; 4]. In oil and gas fields, the production environments are multicomponent [5; 6], and a mixed corrosion mechanism occurs. The proposed division by corrosion types does not take into account the synergistic effect of the presence of several dissolved gases in the environment. The use of expensive materials or several corrosion protection methods significantly increases the cost of pipeline operation.

Based on the corrosion mechanism, a protection method is selected, for example, the material of oil field pipes. According to [7–9], the chemical composition of steel has a significant effect on the process and rate of corrosion: the presence of various alloying elements in steel can both provoke and slow down its destruction under the influence of an aggressive environment. Depending on the composition of the transported medium and the corrosion mechanism, among the materials used, there are chromium-containing steels [10] resistant to pitting carbon dioxide corrosion and steels resistant to stress-corrosion cracking in  $H_2S$ -containing environments [11]. The choice of specific

corrosion-resistant steel depends on factors such as temperature, pressure, concentration of aggressive substances, and the level of mechanical properties. Steels with the addition of chromium, which provides resistance to carbon dioxide corrosion and high strength, are often used for transporting oil and gas.

The behaviour of chromium-containing steel grades in  $H_2S$ -containing environments and the effect of microalloying additives on corrosion resistance have been poorly studied. The significance of the influence of the level of strength properties and the type of microstructure of low-alloy steels on corrosion resistance in environments with  $CO_2$  and  $H_2S$  is unknown.

Taking into account all the above-mentioned operational features and corrosion protection methods, when developing new steels with increased operational reliability, it is necessary to take into account the effect of the complex impact of a multicomponent corrosive environment [12–14], and the behaviour of steels in these environments over time.

The purpose of the work is to determine the influence of the chemical composition, microstructure, and level of mechanical properties of 10KhB, 10F, 10B, 15KhF steels used for linear oil field pipelines on corrosion resistance in complex aggressive environments containing both  $CO_2$  and  $H_2S$ .

## METHODS

### Research materials

The objects of the study were 10KhB, 10F, 10B, and 15KhF steels (Table 1) after volumetric heat treatment in modes ensuring strength properties at the level of K52–K56. The studied steels are characterised by the presence of chromium in the composition in the range of 0.41–0.64 %, which corresponds to the composition of oil and gas pipes resistant to carbon dioxide corrosion. 10KhB steel is additionally microalloyed with niobium, titanium; 10B steel – with niobium; 10F and 15KhF steels – with vanadium.

The steels were smelted under laboratory conditions in a vacuum induction furnace with a capacity of 60 kg. Commercially pure iron (ARMCO), charge blank and ferroalloys were used as charge materials. After melting and casting, cylindrical ingots with a diameter of 150–160 mm and a length of 300–350 mm were subjected to hot

**Table 1.** Content of main alloying elements of experimental pipe steels, mass fraction, %  
**Таблица 1.** Содержание основных легирующих элементов опытных трубных сталей, массовая доля, %

Steel grade	C	Cr	Nb	V	Ti
10KhB	0.07	0.64	0.031	0.002	0.011
10B	0.08	0.42	0.029	0.002	0.007
10F	0.07	0.41	0.005	0.070	0.002
15KhF	0.15	0.54	0.004	0.050	0.006

deformation in the temperature range of 900–1200 °C on a MISIS-130D two-roll piercing mill (Russia) and on a DUO-210 universal longitudinal rolling mill (Russia) to obtain strips with a thickness of 12 mm. Hot-rolled blanks were heated in a laboratory furnace, quenched from a temperature of 910 °C in water, and then tempered at 550–680 °C (duration 30 min).

Table 2 shows the strength, impact toughness and ductility properties of the samples of the studied steels after laboratory heat treatment.

## Methods

Samples for mechanical tests were cut along the rolling direction. Uniaxial tensile tests were performed on an Instron 150 LX universal testing machine (USA) on cylindrical samples with a diameter of 5 mm. Impact bending tests were carried out at a temperature of –60 °C on Charpy samples with a V-shaped notch and a cross section of 10×10 mm using an Instron SI-1M pendulum impact tester (USA).

The structure of the steels was studied by optical microscopy using a ZEISS Axiovert 40 MAT microscope (Germany); corrosion products were analysed using scanning electron microscopy (SEM) on a Tescan Vega SBH3 electron microscope (Czech Republic). X-ray phase analysis of the corrosion products was carried out on a DRON-3 diffractometer (USSR) in  $K_{\alpha}$ –Co radiation.

The steel samples after heat treatment were subjected to corrosion tests, including evaluation of hydrogen-induced cracking resistance according to the NACE TM0284 standard, and sulfide stress-corrosion cracking resistance according to Method A of the NACE TM0177 standard. To evaluate the general corrosion rate, unloaded samples were kept in a model CO<sub>2</sub>- and H<sub>2</sub>S-containing solution for 240 h. The model environment was a solution containing a 5 % NaCl solution of distilled water saturated with a gas cylinder mixture of CO<sub>2</sub> and H<sub>2</sub>S ( $P_{\text{part}}$  of CO<sub>2</sub> was 0.9 atm and  $P_{\text{part}}$  of H<sub>2</sub>S was 0.1 atm), the test temperature was 20 °C. The pH of the solution during the holding varied in the range of 4.3–5.0, and the H<sub>2</sub>S concentration was 93–104 mg/l. The corrosion rate was calculated gravimetrically

by weight loss. The type of corrosion and the form of corrosion damage to the metal were determined using a metallographic method.

## RESULTS

### Metallographic analysis and mechanical properties

The microstructure of the studied 10KhB, 10B, 10F and 15KhF steels after heat treatment according to the “quenching followed by tempering” mode has noticeable differences. This allows evaluating the influence of the chemical composition, namely microalloying additives, on the microstructure parameters and their combined effect on the mechanical properties and corrosion resistance of steel.

From Fig. 1 a, it is evident that the structure of 10KhB steel after heat treatment according to the “quenching + tempering 550 °C” mode is nonequilibrium and is represented by a mixture of ferrite grains of complex shape with tortuous irregular boundaries and lath bainite grains. The proportion of the carbide component is small. The precipitated carbides are finely dispersed and form chains along the boundaries of bainite laths. This type of structure determines the high level of strength properties of steel, corresponding to K56 strength class. The precipitation of a small amount of second phases preserves the alloying elements in the matrix solid solution, therefore, it has a positive effect on the resistance to carbon dioxide corrosion. An increase in the tempering temperature to 600 °C causes a number of structural transformations both in the ferrite matrix and in the carbide component. The structure of the steel after high-temperature tempering at 600 °C is represented by a homogeneous fine-grained ferrite-carbide mixture (Fig. 1 b). The shape of the ferrite grains is preserved from the bainitic structure after hardening and changes slightly as a result of tempering. The carbide component of the structure is uniformly distributed throughout the volume of the metal and includes finely dispersed precipitates of the cementite type of a rounded shape. Inside the ferrite grains, the carbides form chains along the boundaries of the former bainitic laths.

**Table 2.** Mechanical properties of experimental steels after quenching from 910 °C and tempering at 550–680 °C  
**Таблица 2.** Механические свойства опытных сталей после закалки от температуры 910 °C и отпуска 550–680 °C

Steel grade	Tempering temperature, °C	$\sigma_B$ , MPa	$\sigma_T$ , MPa	$\delta_5$ , %	KCV <sup>60</sup> , J/cm <sup>2</sup>
10KhB	550	587	476	21.4	373
	600	554	449	20.5	421
10B	550	578	478	22.3	390
	600	541	440	20.7	397
10F	600	533	433	22.5	383
	680	537	465	20.3	409
15KhF	680	578	476	20.9	326

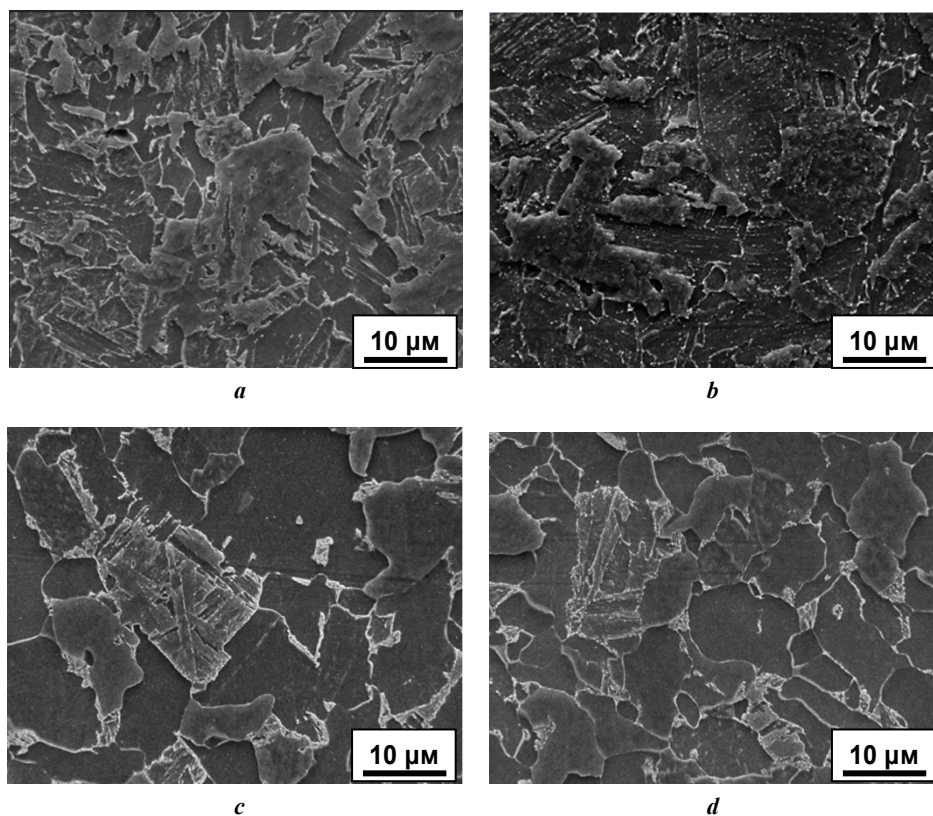


**Fig. 1.** Microstructure of the studied steels:

*a* – 10KhB (quenching + tempering 550 °C); *b* – 10KhB (quenching + tempering 600 °C);  
*c* – 10B (quenching + tempering 550 °C); *d* – 10B (quenching + tempering 600 °C)

**Рис. 1.** Микроструктура исследуемых сталей:

*a* – 10ХБ (закалка + отпуск 550 °C); *b* – 10ХБ (закалка + отпуск 600 °C);  
*c* – 10Б (закалка + отпуск 550 °C); *d* – 10Б (закалка + отпуск 600 °C)

The revealed structural changes reduced the values of the strength properties from the K56 to K54 level. Based on the results of metallographic analysis of the structure of 10KhB steel, it can be assumed that the dispersed cementite carbides formed during tempering at 600 °C partially contain chromium in their composition, however, the remaining chromium in the ferrite matrix should be sufficient to ensure corrosion resistance in CO<sub>2</sub>- and H<sub>2</sub>S-containing environments.

The structure of 10B and 10F steels, shown in Fig. 1 c, d and 2 a, b, respectively, differs from that of 10KhB steel and includes a combination of equiaxed excess ferrite grains and grains with a ferrite-carbide mixture. At the same time, if we compare the morphology of the carbide component for 10KhB, 10F and 10B steels after tempering at 600 °C, a difference in shape and size is noticeable. Carbides in 10KhB steel are dispersed and rounded (Fig. 1 b), while in 10B and 10F steels, they are finely dispersed and have an elongated ellipsoid shape (Fig. 1 d, 2 a).

A comparative analysis of the strength properties and microstructure of 10B steel showed that with an increase in the tempering temperature from 550 to 600 °C, the strength decreases, while no noticeable changes in the structure were detected. Consequently, during tempering, transformations occur in the ferrite matrix at the dislocation level and carbonitride precipitates of microalloying elements are formed. Chromium is retained in the ferrite matrix.

An increase in the tempering temperature of 10F steel to 680 °C had the strongest effect on the shape of the carbide component. Due to the processes of spheroidisation and coagulation, cementite-type carbides acquired a larger and rounded shape. In Fig. 2 b, the result of the process of spheroidisation of carbides along grain boundaries is especially noticeable.

According to the results of uniaxial tensile tests, an increase in the tempering temperature from 600 to 680 °C of 10F steel led to a growth in strength properties. This effect is caused by dispersion strengthening during the precipitation of finely dispersed vanadium carbides. The binding of carbon by vanadium retains most of the chromium in solid solution.

The structure of 15KhF steel differs significantly from other studied steels. The ferrite-carbide structure shown in Fig. 2 c is characterised by a large number of rounded cementite-type precipitates uniformly distributed throughout the volume of the ferrite matrix. Chromium can be part of cementite, therefore, the formed type of microstructure of 15KhF steel reduces corrosion resistance in a CO<sub>2</sub>-containing environment.

Despite the revealed difference in the type of microstructure and the level of strength properties, laboratory corrosion tests in an H<sub>2</sub>S-containing environment using NACE TM0284 and NACE TM0177 standardised methods



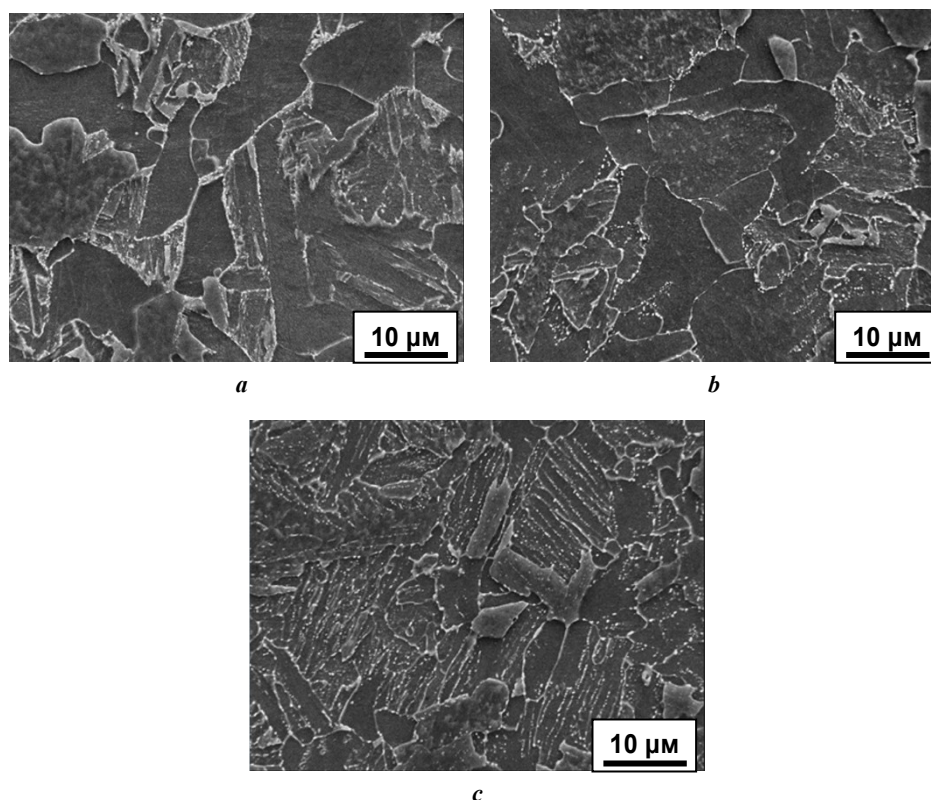


**Fig. 2.** Microstructure of the studied steels:  
**a** – 10F (quenching + tempering 600 °C); **b** – 10F (quenching + tempering 680 °C);  
**c** – 15KhF (quenching + tempering 680 °C)  
**Рис. 2.** Микроструктура исследуемых сталей:  
**a** – 10Ф (закалка + отпуск 600 °C); **b** – 10Ф (закалка + отпуск 680 °C);  
**c** – 15ХФ (закалка + отпуск 680 °C)

showed that the metal of all the steels studied, regardless of microalloying and strength class, has increased resistance to hydrogen cracking (CLR 0 % and CTR 0 %) and a threshold stress of more than 80 %.

### Corrosion properties

The results of corrosion tests of the steel samples in a multicomponent environment containing CO<sub>2</sub> and H<sub>2</sub>S presented in Table 3 indicate an insignificant difference in the corrosion resistance of the steels. The obtained values of the general corrosion rate are in the range of 0.11–

0.14 mm/year. 15KhF steel is characterised by the highest values of the general corrosion rate. Probably, the high density and large size of the alloyed cementite precipitates adversely affect the corrosion resistance.

A visual analysis of the steel samples after exposure in a model environment for 240 h showed that all samples were subjected to uniform corrosion. No pitting corrosion, microcracks or blisterings were detected. Consequently, the main mechanism of corrosion of the low-carbon low-alloy steels in a multicomponent CO<sub>2</sub>- and H<sub>2</sub>S-containing environment is uniform corrosion.

**Table 3.** Results of the assessment of the general corrosion rate in a multicomponent environment depending on the tempering mode of the quenched steels under study

**Таблица 3.** Результаты оценки скорости общей коррозии в многокомпонентной среде в зависимости от режима отпуска закаленных исследуемых сталей

Test objects	10KhB		10B		10F		15KhF
	Tempering 550 °C	Tempering 600 °C	Tempering 550 °C	Tempering 600 °C	Tempering 600 °C	Tempering 680 °C	Tempering 680 °C
Corrosion rate, mm/year*	0.12	0.12	0.12	0.12	0.12	0.11	0.14

Note. \* The measurement error is equal to the numerical uncertainty and is  $\pm 0.01$  mm/year.

Примечание. \* Погрешность измерений равна численно неопределенности и составляет  $\pm 0,01$  мм/год.

As a result of X-ray phase analysis of corrosion products formed on the surface of the samples, it was found that iron sulfide FeS is the main component of the corrosion products formed during exposure to CO<sub>2</sub>- and H<sub>2</sub>S-containing environments. In the X-ray diffraction patterns of all the tested samples, lines corresponding to the sample metal matrix were identified – K-lines of the  $\alpha$ -Fe phase (BCC lattice) and a low-intensity peak corresponding to FeS sulfide – mackinawite (Fig. 3).

Despite the fact that the gas mixture contains only 10 % of H<sub>2</sub>S, its effect on the metal prevails over 90 % of CO<sub>2</sub> and determines the leading corrosion mechanism. The dominance of H<sub>2</sub>S in a multicomponent medium is caused by its greater solubility in an aqueous solution under the studied conditions. The content of H<sub>2</sub>S in the solution is significantly higher than of CO<sub>2</sub>. The product of the interaction of the metal with dissolved H<sub>2</sub>S is sulfide FeS, which is less soluble than FeCO<sub>3</sub> and forms a film on the surface of the samples. Dissolved in the model CO<sub>2</sub> solution also interacts with the metal, but the reaction of carbonate formation is slower than that of sulfides.

The appearance of the corrosion products formed on the surface of all the steel samples studied during the holding time of 240 h indicates the unevenness of the layer (Fig. 4). Comparative analysis of the surface layer does not allow establishing the dependence of the thickness and composition of the corrosion products on the structural state and chemical composition of the steels. The uneven nature of the sulfide film distribution on the surface of samples made of 10B and 10F steels is similar to that of 10KhB steel (Fig. 4 b, c, Table 3). Therefore, the proposed

variants of microalloying systems make it possible to achieve an equally high level of corrosion resistance for the studied low-carbon steels in an environment containing H<sub>2</sub>S and CO<sub>2</sub>. The surface of the samples has an etched relief in which structural elements appear, which indicates the dissolution of iron and the occurrence of corrosion. The etching of the metal by the environment occurs along certain crystallographic planes.

The corrosion products on the surface of 10KhB steel samples after heat treatment using the "quenching and tempering 550 °C" and "quenching and tempering 600 °C" modes are represented by an uneven thin film of iron sulfide. Fig. 5 shows that an increase in the tempering temperature leads to an increase in the number of point corrosion lesions and an increase in the thickness of the corrosion product layer from 2 to 5  $\mu$ m. When examining the sections of 10KhB steel samples, an uneven distribution of the surface film of sulfides of non-uniform thickness was found. Single corrosion lesions up to 5–7  $\mu$ m deep filled with dense deposits were revealed. The corrosion products are characterised by an increased Cr content of up to 1.5 wt. %, which is 2 times higher than the Cr content in the metal. The concentration of S in the corrosion products does not exceed 1 wt. %.

The uniform corrosion mechanism prevails over the pitting one. The main reasons for the formation of local point lesions are a decrease in the strength of the matrix and the formation of large carbide precipitates of the cementite type. The carbide and ferrite matrix form a local galvanic couple, where the carbide has lower solubility and acts as a cathode, and the ferrite acts as an anode.

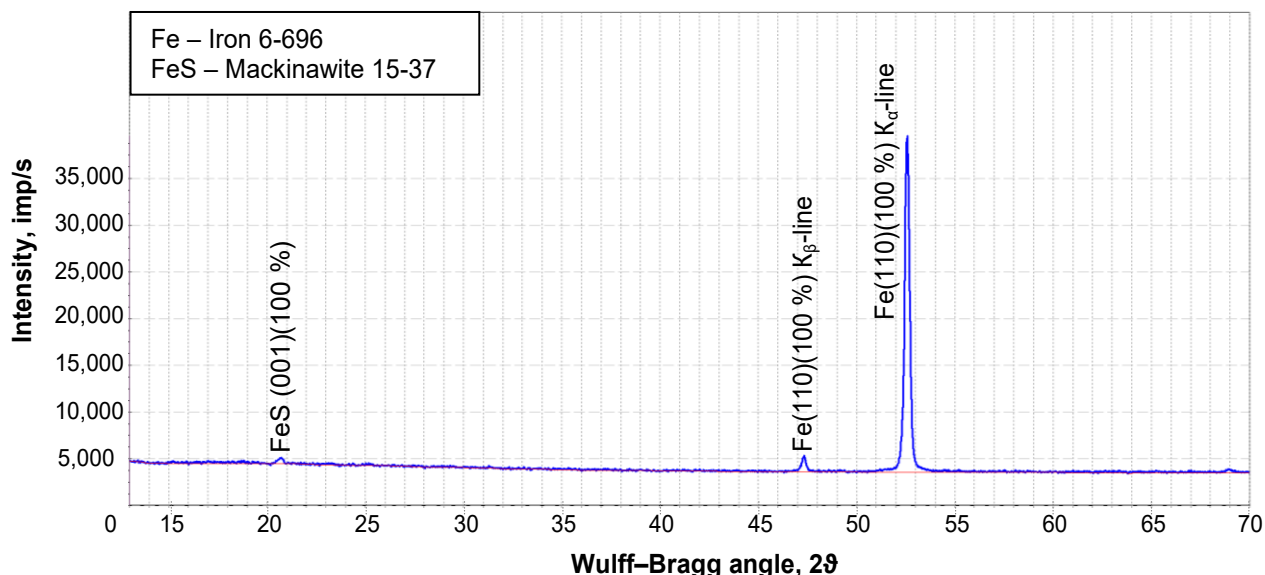
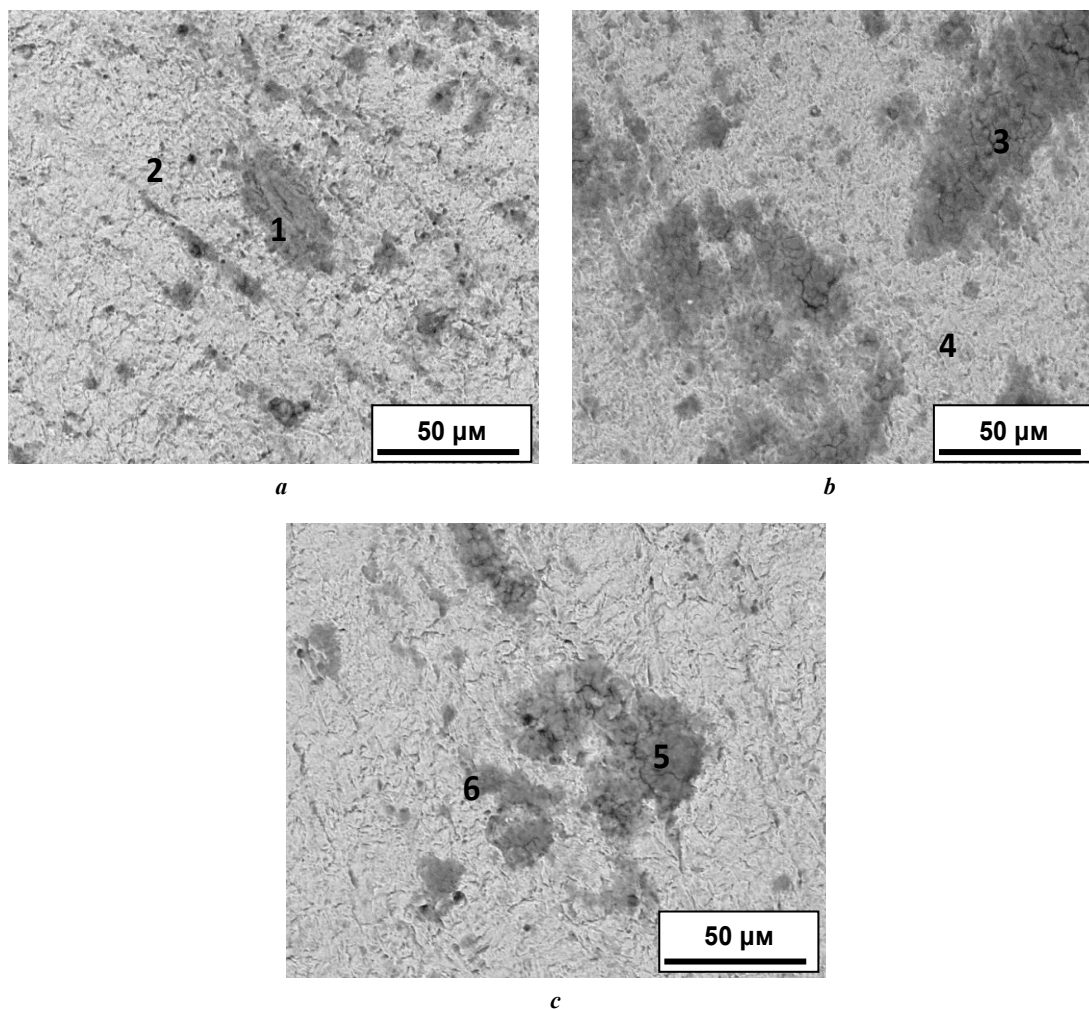


**Fig. 3.** Results of X-ray phase analysis from the surface of samples after testing in CO<sub>2</sub>- and H<sub>2</sub>S-containing environment

**Рис. 3.** Результаты рентгенофазового анализа с поверхности образцов после испытаний в CO<sub>2</sub>- и H<sub>2</sub>S-содержащей среде



No.	O	Si	S	Cr	Mn	Fe
1	11.34	0.43	13.86	1.18	0.69	The rest
2	3.37	0.56	0.92	0.76	1.14	The rest
3	15.98	0.82	3.78	1.04	1.03	The rest
4	3.62	0.53	0.52	0.60	1.30	The rest
5	20.53	0.48	2.90	0.44	0.63	The rest
6	3.48	0.38	0.44	0.57	1.03	The rest

**Fig. 4.** Appearance and composition of corrosion products on the surface of the studied samples: **a** is 10KhB (quenching + tempering 550 °C); **b** is 10B (quenching + tempering 600 °C); **c** is 10F (quenching + tempering 680 °C); **d** is chemical composition of corrosion products

**Рис. 4.** Вид и состав продуктов коррозии на поверхности исследуемых образцов: **a** – 10ХБ (закалка + отпуск 550 °C); **b** – 10Б (закалка + отпуск 600 °C); **c** – 10Ф (закалка + отпуск 680 °C); **d** – химический состав продуктов коррозии

## DISCUSSION

The comparative analysis of the nature of corrosion damage and the composition of corrosion products on the samples of the studied steels showed that during holding in an environment containing CO<sub>2</sub> ( $P_{\text{CO}_2}=0.9$  atm) and H<sub>2</sub>S ( $P_{\text{H}_2\text{S}}=0.1$  atm), the predominant mechanism is uniform sulfide corrosion. Regardless of the composition of the studied steels and strength properties, uniform dissolution

of the metal occurs, as evidenced by the formation of an etched surface relief. A thin iron sulfide film is formed on the surface of the samples, which serves as a barrier to further interaction of the metal with the environment and slows down the corrosion process. For comparison: in [15], the rate of general corrosion after holding in a CO<sub>2</sub>-containing environment without the addition of H<sub>2</sub>S was studied. The obtained values of the rate of general corrosion

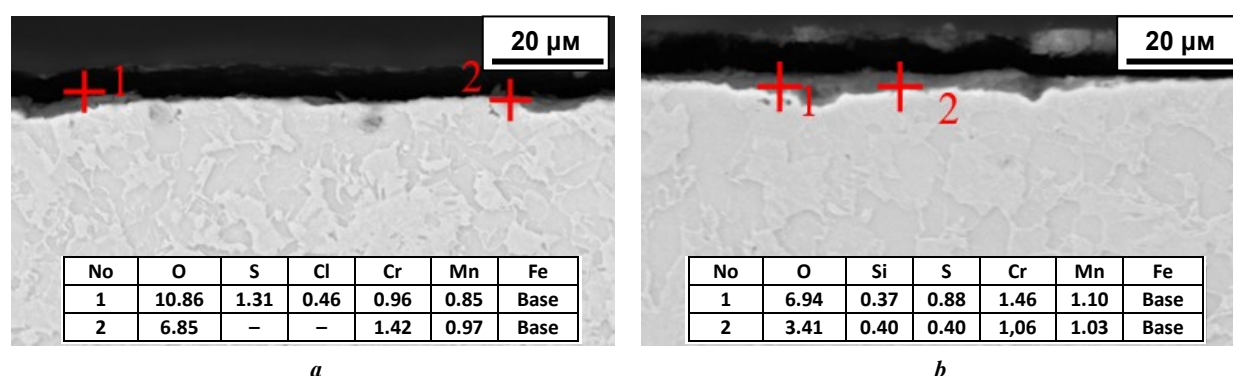


**Fig. 5.** Cross-section of corrosion products of the studied samples:  
*a* – 10KhB (quenching + tempering 550 °C); *b* – 10KhB (quenching + tempering 600 °C)

**Рис. 5.** Сечение продуктов коррозии исследуемых образцов:  
*a* – 10ХБ (закалка + отпуск 550 °C); *b* – 10ХБ (закалка + отпуск 600 °C)

in a CO<sub>2</sub>-containing environment for low-carbon microalloyed steels in some cases are 2 times higher than the corrosion rates obtained in the presented work. In [16], it is shown that the rate of corrosion developing by the sulfide mechanism is lower than the rate of carbon dioxide corrosion. Accordingly, it will be interesting to assess the effect of different concentrations of CO<sub>2</sub> and H<sub>2</sub>S on the corrosion rate. It is important to understand at what H<sub>2</sub>S concentrations in a multicomponent environment the transition to the predominant formation of carbonates and the CO<sub>2</sub> corrosion predominance is possible, since there is still no unambiguous opinion in the literature on the influence of H<sub>2</sub>S additives on the rate of general corrosion and the predominant mechanism.

The low dependence of the rate of general sulfide corrosion on the chemical composition of steels is confirmed by the obtained values of corrosion rates, which are 0.11–0.14 mm/year. It was found that a decrease in the concentration of carbon in steel reduces the corrosion rate. The revealed dependence is associated with the release of a small amount of carbides, which retain the main alloying elements in the matrix. Moreover, in a corrosive environment, carbides form a galvanic couple with the ferrite matrix accelerating the corrosion of the matrix. At the same time, the influence of microalloying of the studied steels, as well as the tempering mode, which determines the amount of carbonitride precipitation in the structure, on the level of the general corrosion rate of microalloyed steels was not revealed. Consequently, for steel of the same chemical composition, varying the tempering temperature mode and changing the composition of the carbide phase, it is possible to regulate the level of strength properties, maintaining a low corrosion rate. In the works [17–20] dealing with the study of corrosion in environments containing CO<sub>2</sub> and H<sub>2</sub>S, only an option for increasing corrosion resistance by introducing microalloying additives is proposed.

Structural transformations occurring in the ferrite matrix during tempering did not affect the rate of general corrosion. Only at the local level by the formation of point lesions with a depth of 5–7 μm was it possible to assess the role of the structural factor in the process of sulfide corrosion. The weak intensity of local corrosion development does not

allow a quantitative comparative assessment of the corrosion resistance of samples with different carbide components. Consequently, at low concentrations of dissolved H<sub>2</sub>S and the presence of CO<sub>2</sub> in the environment, the corrosion rate of low-carbon low-alloy steels weakly depends on the structure and properties of the steel and does not exceed 0.14 mm/year, since it is determined by the rate of formation of the surface iron sulfide film.

The studies showed as well that, regardless of the microalloying additives and the strength level achieved due to different tempering temperatures, high resistance to hydrogen cracking and hydrogen sulfide stress cracking can be achieved in low-carbon steels. It is worth noting that various chemical compositions are used to achieve different levels of strength, cold resistance and resistance to hydrogen sulfide cracking in steels obtained by controlled rolling. Manufacturers are forced to simultaneously support several technologies for the production of rolled products, often using complex expensive combinations of microalloying: niobium and titanium or niobium, vanadium and titanium [20]. Moreover, when manufacturing rolled products using controlled rolling methods, achieving a combination of high cold resistance to –60 °C and resistance to hydrogen cracking is only possible with a carbon content of no more than 0.07 %, which requires additional expensive alloying [20]. During unstable supplies of niobium to the Russian market, it is advantageous and advisable to have technologies and concepts of chemical compositions that allow switching to various microalloying systems without losing any properties of the final product, from strength to corrosion resistance in various environments. In addition, the ability to obtain different strength classes with all other equal pipe manufacturing options is important for pipeline components that are produced in small quantities for the construction of special pipelines.

## CONCLUSIONS

For the developed steel compositions, appropriate tempering regimes ensure both strength classes K52–K56 and high Charpy impact toughness at –60 °C, despite microstructural variations resulting from different alloying systems.



Corrosion tests in accordance with NACE TM0284 and NACE TM0177 confirmed that all studied steels, regardless of alloying system or strength class, exhibited excellent resistance to hydrogen cracking (CLR 0 %, CTR 0 %) and SSC (threshold stress >80 %).

In a model CO<sub>2</sub>-H<sub>2</sub>S environment, the general corrosion rate of the steels was 0.11–0.14 mm/year, independent of alloying system, strength class, or microstructure. In all cases, the dominant corrosion mechanism was uniform H<sub>2</sub>S corrosion, even though the CO<sub>2</sub> partial pressure was significantly higher than that of H<sub>2</sub>S.

## REFERENCES

1. Tkacheva V.E., Brikov A.V., Lunin D.A., Markin A.N. *Lokalnaya CO<sub>2</sub>-korroziiya neftepromyslovogo oborudovaniya* [Localized CO<sub>2</sub> corrosion of oilfield equipment]. Ufa, RN-BashNIPIneft Publ., 2021. 168 p.
2. Tkacheva V.E., Markin A.N., Kshnyakin D.V., Mal'tsev D.I., Nosov V.V. Corrosion of downhole equipment in hydrogen sulfur-containing environments. *Theory and Practice of Corrosion Protection*, 2021, vol. 26, no. 2, pp. 7–26. DOI: [10.31615/j.corros.prot.2021.100.2-1](https://doi.org/10.31615/j.corros.prot.2021.100.2-1).
3. Bregman Dzh. *Ingibitoriy korrozii* [Corrosion inhibitors]. Moscow, Khimiya Publ., 1966. 312 p.
4. Gonik A.A. *Korroziiya neftepromyslovogo oborudovaniya i mery ee preduprezhdeniya* [Corrosion of Oilfield Equipment and Measures to Prevent it]. Moscow, Nedry Publ., 1976. 192 p.
5. Ulig G.G. *Korroziiya i borba s ney. Vvedenie v korrozi-onnyuyu nauku i tekhniku* [Corrosion and corrosion control. An introduction to corrosion science and engineering]. Leningrad, Khimiya Publ., 1989. 456 p.
6. Vyboyshechik M.A., Zyryanov A.O., Gruzkov I.V., Fedotova A.V. Carbon dioxide corrosion of oilfield casing and tubular goods in media saturated with H<sub>2</sub>S and Cl. *Science Vector of Togliatti State University*, 2019, no. 2, pp. 6–17. DOI: [10.18323/2073-5073-2019-2-6-17](https://doi.org/10.18323/2073-5073-2019-2-6-17).
7. Choi Yoon-Seok, Nesic S., Ling Shiun. Effects of H<sub>2</sub>S on the CO<sub>2</sub> corrosion of carbon steel in acidic solutions. *Electrochemical Acta*, 2011, vol. 56, no. 4, pp. 1752–1760. DOI: [10.1016/j.electacta.2010.08.049](https://doi.org/10.1016/j.electacta.2010.08.049).
8. Vyboyshechik M.A., Ioffe A.V. The development of steel resistant to carbon dioxide corrosion in oilfield media. *Perspektivnye materialy*. Tolyatti, Tolyatinskiy gosudarstvennyy universitet Publ., 2017. Vol. 7, pp. 115–166. EDN: [HFOONS](https://elibrary.ru/hfonns).
9. Lopez D.A., Perez T., Simison S.N. The influence of microstructure and chemical composition of carbon and low alloy steels in CO<sub>2</sub> corrosion. A state-of-the-art appraisal. *Materials & Design*, 2003, vol. 24, no. 8, pp. 561–575. DOI: [10.1016/S0261-3069\(03\)00158-4](https://doi.org/10.1016/S0261-3069(03)00158-4).
10. Zhao Xuehui, Li Guoping, Liu Junlin, Li Mingxing, Du Quanqing, Han Yan. Corrosion Performance Analysis of Tubing Materials with Different Cr Contents in the CO<sub>2</sub> Flooding Injection–Production Environment. *Coatings*, 2023, vol. 13, no. 10, article number 1812. DOI: [10.3390/coatings13101812](https://doi.org/10.3390/coatings13101812).
11. Ko M., Ingham B., Laycock N., Williams D.E. In situ synchrotron X-ray diffraction study of the effect of chromium additions to the steel and solution on CO<sub>2</sub> corrosion of pipeline steels. *Corrosion Science*, 2014, vol. 80, pp. 237–246. DOI: [10.1016/j.corsci.2013.11.035](https://doi.org/10.1016/j.corsci.2013.11.035).
12. Sun Jianbo, Sun Chong, Lin Xueqiang, Cheng Xiangkun, Liu Huifeng. Effect of chromium on corrosion behavior of P110 steels in CO<sub>2</sub>-H<sub>2</sub>S environment with high pressure and high temperature. *Materials*, 2016, vol. 9, no. 3, article number 200. DOI: [10.3390/ma9030200](https://doi.org/10.3390/ma9030200).
13. Vagapov R.K., Zapevalov D.N. Aggressive environmental factors causing corrosion at gas production facilities in the presence of carbon dioxide. *Theory and Practice of Corrosion Protection*, 2020, vol. 25, no. 4, pp. 7–17. DOI: [10.31615/j.corros.prot.2020.98.4-1](https://doi.org/10.31615/j.corros.prot.2020.98.4-1).
14. Li Qiang, Jia Wenguang, Yang Kaixiang, Dong Wen-feng, Liu Bingcheng. CO<sub>2</sub> Corrosion Behavior of X70 Steel under Typical Gas-Liquid Intermittent Flow. *Metals*, 2023, vol. 13, no. 7, article number 1239. DOI: [10.3390/met13071239](https://doi.org/10.3390/met13071239).
15. Chen Xuezhong, Yang Xiaomin, Zeng Mingyou, Wang Hu. Influence of CO<sub>2</sub> partial pressure and flow rate on the corrosion behavior of N80 steel in 3.5% NaCl. *International Journal of Electrochemical Science*, 2023, vol. 18, no. 8, article number 100218. DOI: [10.1016/j.ijoes.2023.100218](https://doi.org/10.1016/j.ijoes.2023.100218).
16. Kudashov D.V., Ioffe A.V., Naumenko V.V., Muntin A.V., Udod K.A., Kovtunov S.V. Corrosion resistance of welded tubing of L80 strength group of different chemical composition. *Izvestiya vuzov. Chernaya metallurgiya*, 2022, vol. 65, no. 3, pp. 200–208. DOI: [10.17073/0368-0797-2022-3-200-208](https://doi.org/10.17073/0368-0797-2022-3-200-208).
17. Popkova Yu.I., Grigorev A.Ya. Influence of steel characteristics on the corrosion resistance of tubing under carbon dioxide corrosion conditions. *Bulletin Sukhoi State technical university of Gomel*, 2024, no. 1, pp. 48–62. DOI: [10.62595/1819-5245-2024-1-48-62](https://doi.org/10.62595/1819-5245-2024-1-48-62).
18. Amezhnov A.V., Rodionova I.G., Gladchenkova Yu.S., Zarkova E.I., Stukalova N.A. Comparative assessment of the aggressiveness of various mediums. Influence of medium characteristics on the rate and mechanisms of corrosion processes. *Problems of ferrous metallurgy and materials science*, 2020, no. 3, pp. 62–70. EDN: [HBIWWB](https://elibrary.ru/hbiwwb).
19. Benedito A.V., Torres C.A.B., Silva R.M.C., Krahel P.A., Cardoso D.C.T., Silva F.A., Martins C.H. Effects of niobium addition on the mechanical properties and corrosion resistance of microalloyed steels: a review. *Buildings*, 2024, vol. 14, no. 5, article number 1462. DOI: [10.3390/buildings14051462](https://doi.org/10.3390/buildings14051462).
20. Kholodnyi A.A. Resistance increase to hydrogen-induced sheet cracking for gas and oil pipes based on the structure formation control in the central segregation zone. *Steel in translation*, 2020, vol. 50, no. 1, pp. 53–61. DOI: [10.3103/S0967091220010052](https://doi.org/10.3103/S0967091220010052).

## СПИСОК ЛИТЕРАТУРЫ

1. Ткачева В.Э., Бриков А.В., Лунин Д.А., Маркин А.Н. Локальная CO<sub>2</sub>-коррозия нефтепромыслового оборудования. Уфа: РН-БашНИПИнефть, 2021. 168 с.
2. Ткачева В.Э., Маркин А.Н., Кшнякин Д.В., Мальцев Д.И., Носов В.В. Коррозия внутрискважинного оборудования в сероводородсодержащих средах // Практика противокоррозионной защиты. 2021. Т. 26. № 2. С. 7–26. DOI: [10.31615/j.corros.prot.2021.100.2-1](https://doi.org/10.31615/j.corros.prot.2021.100.2-1).



3. Брегман Дж. Ингибиторы коррозии. М.: Химия, 1966. 312 с.
4. Гоник А.А. Коррозия нефтепромыслового оборудования и меры ее предупреждения. М.: Недры, 1976. 192 с.
5. Улиг Г.Г. Коррозия и борьба с ней. Введение в коррозионную науку и технику. Л.: Химия, 1989. 456 с.
6. Выбойщик М.А., Зырянов А.О., Грузков И.В., Федотова А.В. Углекислотная коррозия нефтепромысловых труб в средах, насыщенных  $H_2S$  и  $Cl$  // Вектор науки Тольяттинского государственного университета. 2019. № 2. С. 6–17. DOI: [10.18323/2073-5073-2019-2-6-17](https://doi.org/10.18323/2073-5073-2019-2-6-17).
7. Choi Yoon-Seok, Nesic S., Ling Shiun. Effects of  $H_2S$  on the  $CO_2$  corrosion of carbon steel in acidic solutions // *Electrochemical Acta*. 2011. Vol. 56. № 4. P. 1752–1760. DOI: [10.1016/j.electacta.2010.08.049](https://doi.org/10.1016/j.electacta.2010.08.049).
8. Выбойщик М.А., Иоффе А.В. Разработка стали, стойкой к углекислотной коррозии в нефтедобываемых средах // Перспективные материалы. Т. 7. Тольятти: Тольяттинский государственный университет, 2017. С. 115–166. EDN: [HFONNS](https://www.edn.ru/HFONNS).
9. Lopez D.A., Perez T., Simison S.N. The influence of microstructure and chemical composition of carbon and low alloy steels in  $CO_2$  corrosion. A state-of-the-art appraisal // *Materials & Design*. 2003. Vol. 24. № 8. P. 561–575. DOI: [10.1016/S0261-3069\(03\)00158-4](https://doi.org/10.1016/S0261-3069(03)00158-4).
10. Zhao Xuehui, Li Guoping, Liu Junlin, Li Mingxing, Du Quanqing, Han Yan. Corrosion Performance Analysis of Tubing Materials with Different Cr Contents in the  $CO_2$  Flooding Injection–Production Environment // *Coatings*. 2023. Vol. 13. № 10. Article number 1812. DOI: [10.3390/coatings13101812](https://doi.org/10.3390/coatings13101812).
11. Ko M., Ingham B., Laycock N., Williams D.E. In situ synchrotron X-ray diffraction study of the effect of chromium additions to the steel and solution on  $CO_2$  corrosion of pipeline steels // *Corrosion Science*. 2014. Vol. 80. P. 237–246. DOI: [10.1016/j.corsci.2013.11.035](https://doi.org/10.1016/j.corsci.2013.11.035).
12. Sun Jianbo, Sun Chong, Lin Xueqiang, Cheng Xiangkun, Liu Huifeng. Effect of chromium on corrosion behavior of P110 steels in  $CO_2$ - $H_2S$  environment with high pressure and high temperature // *Materials*. 2016. Vol. 9. № 3. Article number 200. DOI: [10.3390/ma9030200](https://doi.org/10.3390/ma9030200).
13. Вагапов Р.К., Запелалов Д.Н. Агрессивные факторы эксплуатационных условий, вызывающие коррозию на объектах добычи газа в присутствии диоксида углерода // Практика противокоррозионной защиты. 2020. Т. 25. № 4. С. 7–17. DOI: [10.31615/j.corros.prot.2020.98.4-1](https://doi.org/10.31615/j.corros.prot.2020.98.4-1).
14. Li Qiang, Jia Wenguang, Yang Kaixiang, Dong Wenfeng, Liu Bingcheng.  $CO_2$  Corrosion Behavior of X70 Steel under Typical Gas-Liquid Intermittent Flow // *Metals*. 2023. Vol. 13. № 7. Article number 1239. DOI: [10.3390/met13071239](https://doi.org/10.3390/met13071239).
15. Chen Xuezhong, Yang Xiaomin, Zeng Mingyou, Wang Hu. Influence of  $CO_2$  partial pressure and flow rate on the corrosion behavior of N80 steel in 3.5% NaCl // *International Journal of Electrochemical Science*. 2023. Vol. 18. № 8. Article number 100218. DOI: [10.1016/j.ijoes.2023.100218](https://doi.org/10.1016/j.ijoes.2023.100218).
16. Кудашов Д.В., Иоффе А.В., Науменко В.В., Мунтин А.В., Удод К.А., Ковтунов С.В. Исследование коррозионной стойкости сварных насосно-компрессорных труб группы прочности L80 различного химического состава // Известия высших учебных заведений. Черная металлургия. 2022. Т. 65. № 3. С. 200–208. DOI: [10.17073/0368-0797-2022-3-200-208](https://doi.org/10.17073/0368-0797-2022-3-200-208).
17. Попкова Ю.И., Григорьев А.Я. Влияние состава стали на коррозионную стойкость насосно-компрессорных труб в условиях углекислотной коррозии // Вестник Гомельского государственного технического университета им. П.О. Сухого. 2024. № 1. С. 48–62. DOI: [10.62595/1819-5245-2024-1-48-62](https://doi.org/10.62595/1819-5245-2024-1-48-62).
18. Амежнов А.В., Родионова И.Г., Гладченкова Ю.С., Заркова Е.И., Стукалова Н.А. Сравнительная оценка агрессивности различных сред. Влияние характеристик среды на скорость и механизмы протекания коррозионных процессов // Проблемы черной металлургии и материаловедения. 2020. № 3. С. 62–70. EDN: [HBIWWB](https://www.edn.ru/HBIWWB).
19. Benedito A.V., Torres C.A.B., Silva R.M.C., Krahel P.A., Cardoso D.C.T., Silva F.A., Martins C.H. Effects of niobium addition on the mechanical properties and corrosion resistance of microalloyed steels: a review // *Buildings*. 2024. Vol. 14. № 5. Article number 1462. DOI: [10.3390/buildings14051462](https://doi.org/10.3390/buildings14051462).
20. Холодный А.А. Повышение сопротивления водородному растрескиванию листов для газо- и нефтепроводных труб на основе управления структурообразованием в центральной сегрегационной зоне // Сталь. 2020. № 1. С. 46–53. EDN: [EMNGDD](https://www.edn.ru/EMNGDD).

## Влияние термической обработки на структуру и коррозионные свойства микролегированных трубных сталей с содержанием хрома до 1 %

**Чистопольцева Елена Александровна**<sup>1,5</sup>, кандидат технических наук,  
руководитель департамента специального материаловедения  
**Кудашов Дмитрий Викторович**<sup>2,6</sup>, кандидат технических наук, директор  
**Комиссаров Александр Александрович**<sup>3,7</sup>, кандидат технических наук,  
заведующий лабораторией «Гибридные наноструктурные материалы»  
**Ющук Вячеслав Васильевич**<sup>3,8</sup>, инженер научного проекта  
**Мунтин Александр Вадимович**<sup>4</sup>, кандидат технических наук,  
директор инженерно-технологического центра  
**Червонный Алексей Владимирович**<sup>4</sup>, кандидат технических наук,  
начальник отдела по исследованиям и разработкам  
**Долгач Егор Дмитриевич**<sup>3</sup>, инженер научного проекта

<sup>1</sup>ООО «ИТ-Сервис», Самара (Россия)

<sup>2</sup>Выксунский филиал НИТУ «МИСИС», Выкса (Россия)

<sup>3</sup>Университет науки и технологий МИСИС, Москва (Россия)

<sup>4</sup>АО «Выксунский металлургический завод», Выкса (Россия)

\*E-mail: chistopolceva@its-samara.com

<sup>5</sup>ORCID: <https://orcid.org/0009-0002-5587-287X>

<sup>6</sup>ORCID: <https://orcid.org/0000-0002-7661-1591>

<sup>7</sup>ORCID: <https://orcid.org/0000-0002-8758-5085>

<sup>8</sup>ORCID: <https://orcid.org/0000-0002-3015-1235>

Поступила в редакцию 22.04.2025

Пересмотрена 20.05.2025

Принята к публикации 17.07.2025

**Аннотация:** Осложнение условий эксплуатации, заключающееся в повышении агрессивности сред за счет присутствия одновременно растворенного сероводорода, углекислого газа, хлоридов, увеличения содержания водной фазы, приводит к значительному сокращению продолжительности безаварийной работы трубопроводов. Ограниченность способов защиты вынуждает использовать одновременно несколько антикоррозионных мероприятий для трубопроводов со сложными средами. В работе предложены системы микролегирования низкоуглеродистых марок сталей 10ХБ, 10Ф, 10Б, 15ХФ с содержанием хрома до 1 % для бесшовных труб и режимы термической обработки, позволяющие достичь одновременно повышенную прочность, хладостойкость и коррозионную стойкость в средах, содержащих  $\text{CO}_2$  и  $\text{H}_2\text{S}$ . По результатам механических испытаний сталей после термической обработки установлено, что предложенные варианты микролегирования гарантируют прочностные свойства классов прочности К52–К56 и хладостойкость одновременно. Морфология карбидной составляющей структуры зависит от микролегирующего элемента и определяет уровень прочности стали, но не оказывает влияния на коррозионную стойкость. Исследуемые стали обладают повышенной стойкостью к водородному растрескиванию и сульфидному коррозионному растрескиванию под напряжением. После выдержки в многокомпонентной  $\text{CO}_2$ - и  $\text{H}_2\text{S}$ -содержащей среде формируется поверхностная пленка сульфида железа, свидетельствующая о протекании равномерной сульфидной коррозии. Скорость коррозии исследуемых сталей и тип коррозии определяются составом агрессивной среды и скоростью формирования поверхностной пленки сульфида железа. Полученные результаты позволяют расширить область применения предлагаемых сталей в многокомпонентных агрессивных средах независимо от вида микролегирования.

**Ключевые слова:** низкоуглеродистая микролегированная сталь; термическая обработка; коррозионно-стойкая бесшовная труба;  $\text{CO}_2$ - и  $\text{H}_2\text{S}$ -содержащая среда; сульфидная коррозия стали; мелкозернистая структура; нефтепромысловые трубопроводы.

**Благодарности:** Работа выполнена в рамках комплексного проекта по теме «Разработка и внедрение комплексных технологий производства бесшовных труб из сталей нового поколения с управляемой коррозионной стойкостью при осложненных условиях эксплуатации для топливно-энергетического комплекса Российской Федерации» в рамках соглашений № 075-11-2023-011 от 10.02.2023 и № 075-11-2025-017 от 27.02.2025 по постановлению Правительства РФ № 218 от 09.04.2010.

**Для цитирования:** Чистопольцева Е.А., Кудашов Д.В., Комиссаров А.А., Ющук В.В., Мунтин А.В., Червонный А.В., Долгач Е.Д. Влияние термической обработки на структуру и коррозионные свойства микролегированных трубных сталей с содержанием хрома до 1 % // Frontier Materials & Technologies. 2025. № 3. С. 101–111. DOI: 10.18323/2782-4039-2025-3-73-8.